HEFAT2014
10th International Conference on Heat Transfer, Fluid Mechanics and Thermodynamics
6 – 9 July 2014
Orlando, Florida

THERMAL CHARACTERISATION ANALYSIS OF HEAT-SINK HEAT PIPES UNDER FORCED CONVECTION

Jung-Chang Wang
Department of Marine Engineering,
National Taiwan Ocean University (NTOU),
Keelung, 20224,
Taiwan R.O.C.,
E-mail: jcwang@ntou.edu.tw

ABSTRACT

The thermal performance of embedded heat pipes heat sink cooling system presents a viable active method for reducing peak operating temperatures of the heat source. This type of embedded heat pipes heat sink module successively transfer heat from a heat source to the heat pipes, the heat sink and their surroundings, and are suitable for cooling electronic systems via forced convection mechanism. The main purpose of this study is to establish a theoretical model that is based on the performance of embedded heat pipes heat sink under different wind speeds and heater areas, and calculate the heat flow of individual embedded heat pipe employed the least smoothing square method and the thermal performance experiment. The computer core of heat-sink heat pipes thermal module (HSHPTM) program applies the theoretical thermal resistance analytical approach with iterative convergence stated in the present study to obtain numerical solution. The results show that this calculating error comparison with experimental results is within ±5%. This HSHPTM has the advantage of rapidly calculating the thermal performance of a heat sink-heat pipes thermal module installed with processor horizontally by inputting simple parameters. The result of this work is a useful thermal management method to facilitate rapid analysis.

INTRODUCTION

With the advances in computer manufacturing industry, integral circuit design is getting more and more complex so that electronic components are made towards the small size and high efficiency development. The central processor unit (CPU), for example, is continued in improving the performance of the chip, but the size still has not changed, which means more transistors are put in the same area to generate more heat per area of electronic component. Thus, the cooling problems of electronic device are increasingly important. Air cooling module with simple aluminum heat sink and fan is to solve the problem of CPU heat load. Increasing the thermal efficiency of thermal module is to transfer more and more heat flow. Adding the fan speed can quickly take away more heat, but also produce a noise problem and the effect is not good. Nowadays, Technical development related with the application of two-phase flow heat transfer assembly to thermal modules has become mature. One of the best selections is the heat pipe-based thermal module. The cooling product of combining the heat pipe and heat sink is the most widely approach [1-8].

The difference between heat-sink heat pipes and traditional heat sink thermal modules is that most of the heat firstly transfers to the evaporator of heat pipe, so that the liquid working fluid vaporizes. The vapour then rises along the heat pipes, releases the heat in the condenser, then turns into liquid, and falls back to the evaporator which is driven by evaporation of the heat pipe produces steam. Steam releases heat in the condensation and re-condenses into liquid backing to the evaporator driving by the capillary force of capillary structure to complete the cycle; and the rest of the heat take away from heat sink through forced convection of fan. Therefore, the heat-sink heat pipe thermal module has better thermal performance at the same rotational speed of fan and produces less noise [9-13]. The embedded heat pipes-heat sink thermal module studied in the present study is shown in Fig.1. This study thus used the superposition method and least smoothing square method to calculate the heat carried to the fins through the base plate and embedded heat pipes, in order to find the ratio of total heat transferred through the embedded heat pipes. These individual thermal resistances of contact, base plate, and base to heat pipes, heat pipes, fins and the total thermal resistance may then be obtained through thermal resistance analysis and the least smoothing square and superposition methods [14-19].

NOMENCLATURE

Q	[Watt]	heat transfer rate
R	[K/W]	Thermal resistance
T	[K]	Temperature

Subscripts

a	Ambient
b	Base plate
f	Fin
s	Source of heat

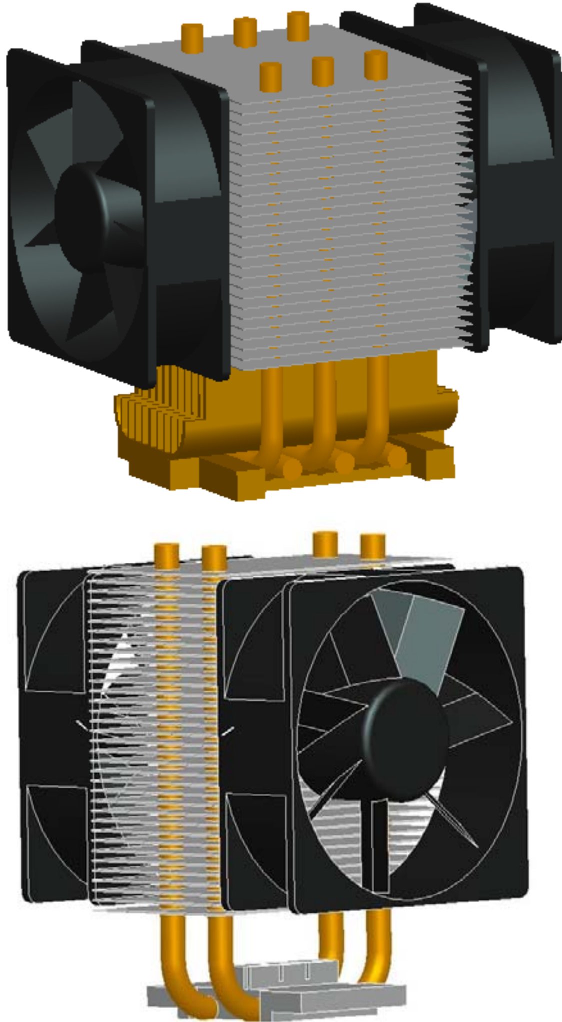

Figure 1 Embedded heat pipes-heat sinks thermal modules

EXPERIMENTAL SET UP

Let the thermal module place on a dummy heater and connect to all apparatus as shown in Figure 2. Dummy heater is an area of 30 mm × 30 mm copper heating block internal heat generated by electronic-resistance heating. By adjusting the power supply to control heating power and increase to 300 W step of 30 W. Two fans were installed on each side of the module to be operated at same air flow direction and rotational speed. The dimensions of the fan are 80 mm × 80 mm × 25 mm. Operating voltage and current are 12 V and 0.24 A. There are three fan speeds of 1000 RPM, 2000 RPM and 3000 RPM. Figure 3 shows the location of each temperature sensor installed in this embedded heat pipe heat sink. T_s is the temperature of heat source, T_b is the temperature of based plate, T_{bu} is the temperature of upper based plate, $T_{hpe,n}$ are the temperatures of evaporator of six heat pipes, $T_{hpc,n}$ are the temperatures of condenser of six heat pipes and T_a is ambient temperature. The symbol n denotes the number and its corresponding location of each temperature sensor attached to the heat pipes as shown in Fig. 3. Heat transferred from heat source to the lower surface of based plate is divided into two parts. The first part is the bypass heat flow Q_b transferring through based plate and heat sink above based plate. The other bypass heat flows Q (1~6) transfer heat from based plate to the six heat pipes embedded asymmetrically into based plate. Then, heat transfers from the evaporator of heat pipe to the condenser and fins and dissipates in the ambient through the forced convection of two fans. Every bypass heat flow Q (1~6) can be estimated by the experiment of cutting heat pipes and superposition principle. Figure 4 shows the experimental thermal resistances network. The R_{if} is the interface resistance. The R_b is based plate thermal resistance. The R_{ba} is based plate convection resistance. The $R_{bhp,n}$ is based plate heat pipe thermal resistance. The $R_{hp,n}$ is heat pipe resistance. The $R_{hpa,n}$ is heat pipe convection resistance. And the R_t is total thermal resistance. Equations (1) and (2) are the definition of experimental thermal resistances in the article.

$$Q = Q_b + \sum_{n=1}^{2or6} Q_n \qquad (1)$$

$$R_t = R_{if} + \frac{1}{\frac{1}{(R_b + R_{hs})} + \sum_{n=1}^{2or6}\left(\frac{1}{R_{bh,n} + R_{h,n} + R_{f,n}}\right)} \qquad (2)$$

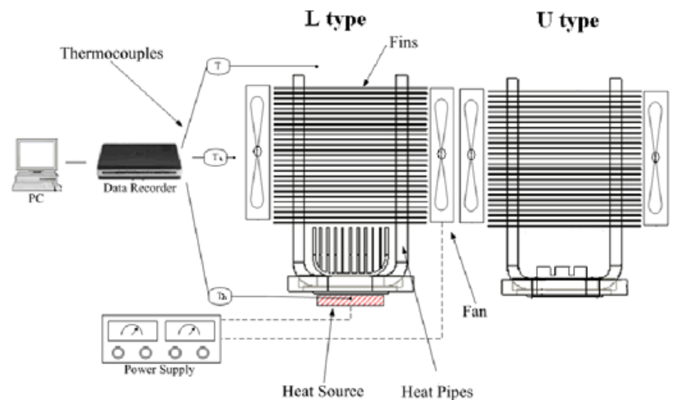

Figure 2 Experimental apparatus

The experimental steps are divided into six parts in the article. The first step involves experimental apparatus calibration and place. The second step is coating thermal grease between the upper surface of dummy heater and the lower surface of based plate. The third step is to fix the dummy heater and thermal module through jig. The fourth step is to turn on the power supply, set the power output of the dummy heater to 30 W, and adjust the fan speed to 1000 RPM. The fifth step is to record the steady-state temperatures through recorder of GL800. The sixth step is to repeat the fifth step with different power outputs at 60 W、90 W、120 W、150 W、180 W、210 W、240 W、270

W、300 W and two other fan speeds at 2000 and 3000 RPM. According to Ref. [13, 15], Eqs. (1) and (2) are concluded with analysing Q_1 to Q_6. And the theoretical heat pipe thermal resistance from Ref. [13, 15] can be revealed through the temperature difference between $T_{hpe,n}$ and $T_{hpc,n}$. Table 1 shows the ratio of bypass heat transfer rate (and thus the heat capacity of heat pipes) at each location to the total heat transfer rate to the entire module which were calculated based on Newton's method.

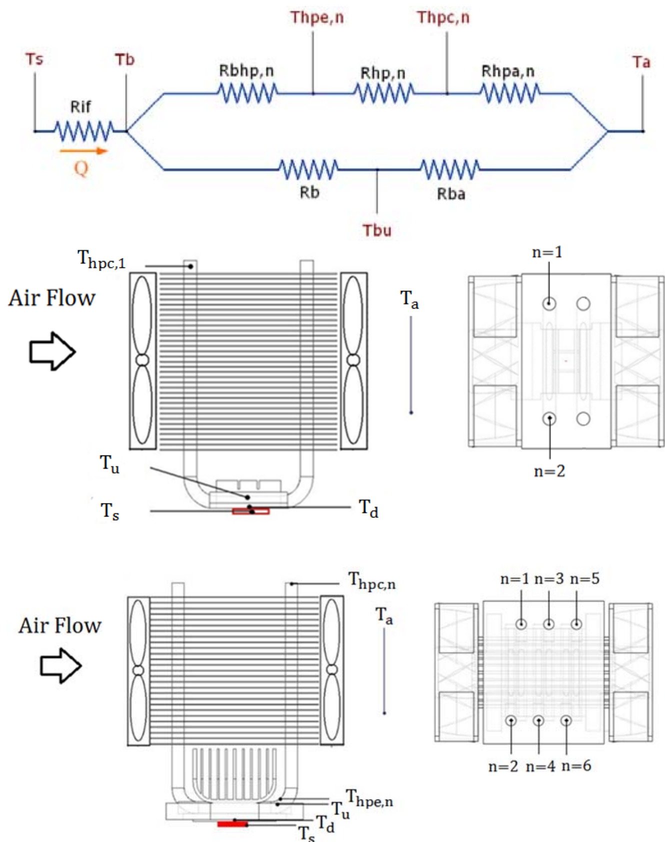

Figure 3 Location of temperature sensors

Table 1 Ratio of bypass heat to total power

Speed(RPM)	1000	2000	3000
Q_1/Q(%)	17.4	15.8	16
Q_2/Q(%)	17.6	15.9	15.1
Q_3/Q(%)	17	15.5	15.2
Q_4/Q(%)	5.2	6.8	11
Q_5/Q(%)	5	5.2	6.9
Q_6/Q(%)	15.9	15.2	15.4

HSHPTM WINDOW PROGRAM

This window program named HSHPTM was coded with Microsoft® Visual Basic™ 6.0 to calculate the thermal performance of a heat sink-heat pipes thermal module in this paper. A numerical solution approach was followed as pure analytical solutions for the thermal governing equations proved to be elusive. From the energy conservation principle, the total heating power Q equals the sum of base plate heat Q_b^i and embedded heat pipes heat Q_j^i . Due to the anticipated large number of case study investigations, which were required to thermally characterise the model problem, problem specific algorithms were developed and the ratio of Q_b^i and Q_j^i to total Q are shown in Ref. [14]. For keeping regularity, the symbols i and j respectively denote the number and location of the embedded heat pipes as in the reference [13, 15]. The total heating power Q equals the sum of the base plate heat Q_b^i and embedded heat pipes heat Q_j^i from the superposition method. The related derivation processes are similar to those shown in Ref. [14]. In order to avoid repetition, they are not shown in this manuscript.

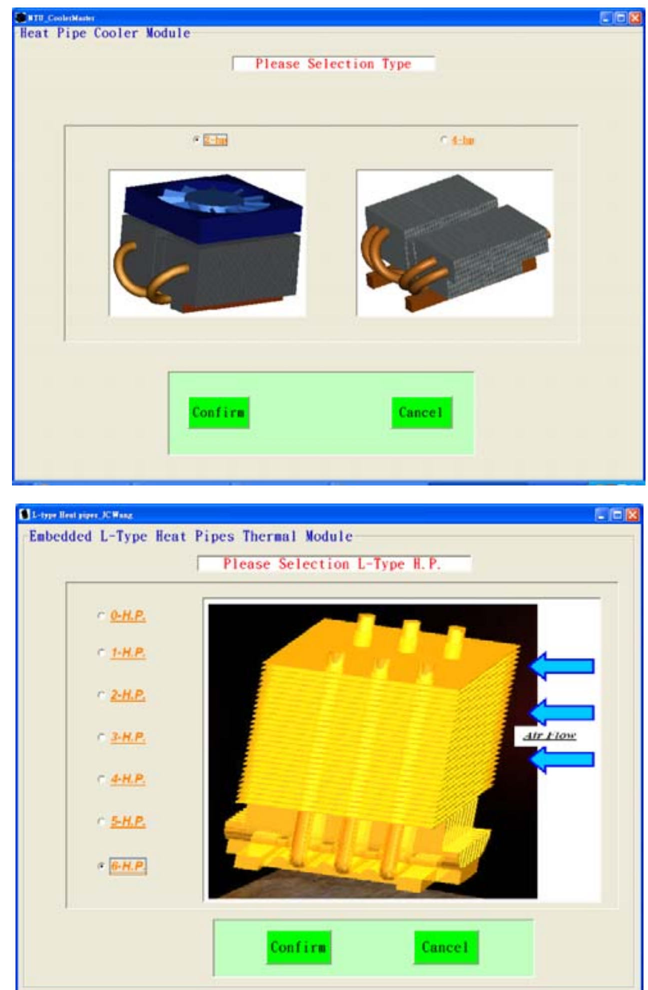

Figure 4 Selection heat sink-heat pipes thermal module type window

Finally, these numerical values, including the individual thermal resistances and temperatures of the heat sink-heat pipes thermal module and heat of the base plate and embedded heat pipes, are obtained through the window program HSHPTM in this paper as shown in Fig. 4. These parameters affect the thermal performance of the heat sink-heat pipes thermal module including the dimensions, thermal performance, and location of the embedded heat pipes. Thus, it is very important for the optimum parameters to be selected to achieve the best thermal performance of the heat sink-heat pipes thermal module. The HSHPTM program contains two main windows. The first is the selection window adjusted in the program as the main menu. In this window, the type of heat sink-heat pipes thermal module can be chosen separately. The second window has five main sub-windows. There are four sub-windows for the input parameters of the thermal module. The first sub-window is the simple parameters of the heat pipes including the dimensions and thermal performance. The second sub-window has the details of the dimensions of a heat sink. The third and fourth sub-windows are the simple parameters containing the input power of the heat source, thermal grease and solder materials, and the performance curve of the fan. All the input parameters required for the study of the window program are given and the window program starts. Later, the HSHPTM program examines the situation by pressing the calculate icon. The fifth sub-window is the window showing the simulation results. In this sub-window, the calculate icon is pressed for analyzing the thermal performance of a heat sink-heat pipes thermal module. This HSHPTM V1.0 utilizes theoretical thermal resistance to estimate the thermal performance of the heat sink-heat pipes thermal module.

DISCUSSION AND RESULTS

Figure 5 shows the experimental interface thermal resistance R_{if} of about 0.1 (K/W), a constant value with no significant difference as the function of the input power. Thermal interface materials (high thermal conductivity) can also have a significant role in lowering interface thermal resistance. The contact thermal resistance is approximately 0.1 ºC/W when the heating power is between 30 W and 300 W. The magnitude of the thermal contact resistance can have a major role in thermal management of electronic devices and, hence, may significantly affect thermal performance of such thermal module. Surface roughness properties and contact pressure as well as mechanical and thermal material properties between two contact surfaces can have a significant effect on the magnitude of thermal contact resistance. Therefore, the interface thermal resistance R_{if} in the present experiment may be treated as a constant. This is because that the thermal conductivity of thermal grease is the same when there is not much change in temperature.

Total thermal resistances are lower at high fan speeds and the thermal module has better thermal performance at higher fan speeds as shown in Fig. 6. This is because of the heating power increasing to the point that the embedded heat pipes are starting to function, and the total thermal resistance shows a decreasing trend. When the rotational speeds of fans are 2000 RPM and 3000 RPM, the total thermal resistances have small changes. The reason is that when the module is running at high fan speeds, the air would be in the turbulent flow regime which possesses higher convective heat transfer coefficient and thus would allow the heat to be removed by the air from the module more quickly. However, the total thermal resistances are getting lower with inducing input power at fan speeds of 1000 RPM resulting from the function of embedding heat pipes. And the total thermal resistance has the lowest value of 0.26 (K/W).

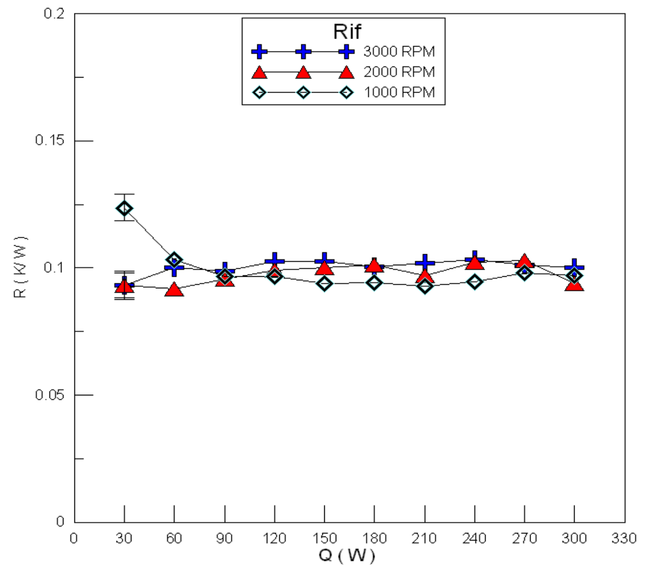

Figure 5 Interface thermal resistances

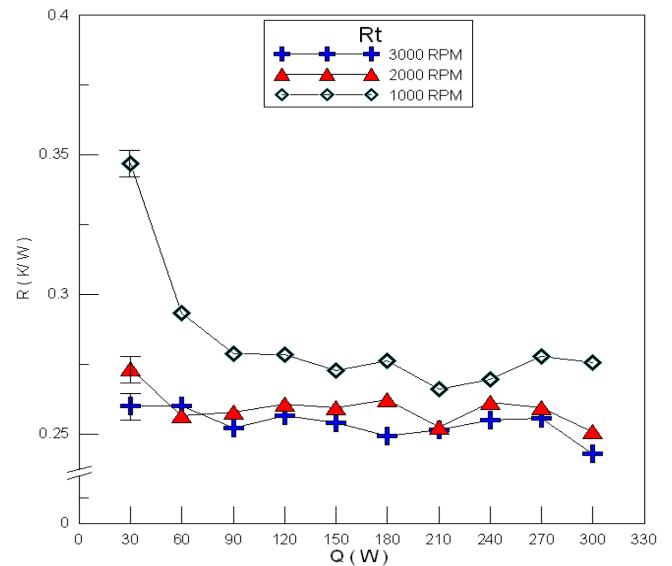

Figure 6 Total thermal resistances

Figure 7 shows the based pate thermal resistances. Because these thermal physical properties of the solid base plate without embedded heat pipes are constant values when the temperature does not change very much, the thermal resistance curves on the paths are horizontal lines which is independent from the increase

of heating power. Figure 8 shows the convection thermal resistances. Much emphasis in heat sink design is spent looking at fin efficiency. The fin efficiency depends on heat transfer coefficient. The fan should be kept above a certain speed to obtain better heat diffusion.

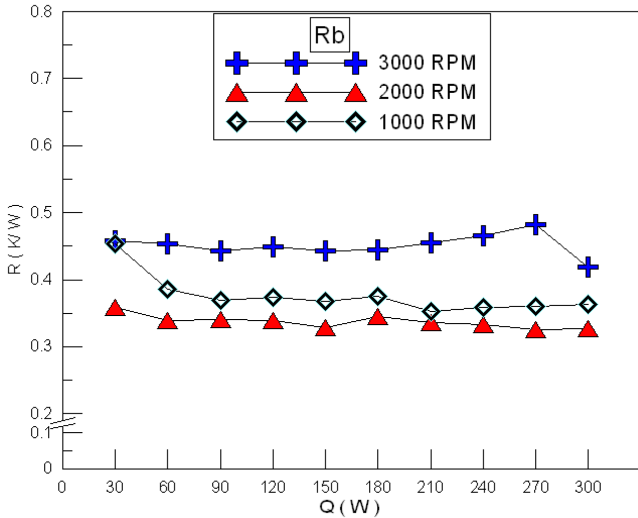

Figure 7 Based plate thermal resistances

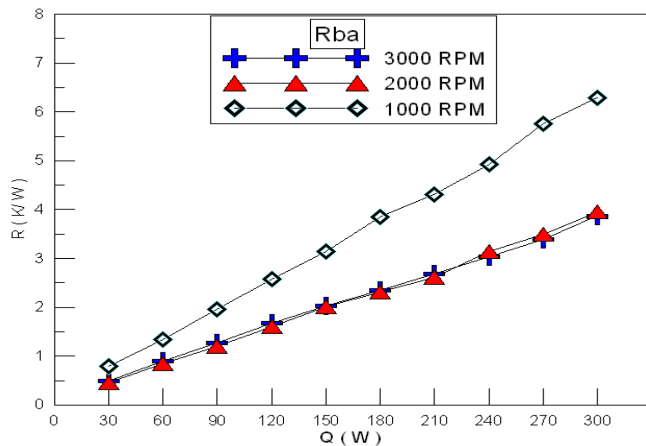

Figure 8 Convection thermal resistances

The present experiment partially focuses on estimating the bypass heat flow. The rest thermal resistances of Tables 2-4 reveal the embedded heat pipes thermal resistances through Table 1 and thermal resistance analysis in the present study. From the tables, the thermal performances of embedded heat pipes are induced and their thermal resistances are lowered with input power increase. However, in theory, a reduction to the heat source area will increase the ratio of the total area of the contact area of the heat pipe to the heat source, thus the bypass heat flow ratio will rise as the heat source area is decreased. These base plate to heat pipes thermal resistances R_{bhp} are shown as Tables 5-7. The embedded heat pipes can dissipate more heat than the base plate. And the convection heat pipes thermal resistances R_{hpa} are shown in Tables 8-10.

Table 2 Embedded heat pipes resistances at 3000 RPM

3000 (RPM)						
Q(W)	R_{hp1}	R_{hp2}	R_{hp3}	R_{hp4}	R_{hp5}	R_{hp6}
30	0.250	0.287	0.285	0.212	0.338	0.238
60	0.250	0.242	0.252	0.151	0.289	0.194
90	0.250	0.228	0.219	0.121	0.209	0.173
120	0.229	0.204	0.186	0.106	0.217	0.173
150	0.212	0.185	0.175	0.097	0.183	0.160
180	0.194	0.176	0.153	0.090	0.169	0.151
210	0.187	0.167	0.144	0.077	0.158	0.142
240	0.171	0.154	0.137	0.072	0.151	0.138
270	0.187	0.152	0.134	0.067	0.139	0.141
300	0.158	0.140	0.122	0.059	0.132	0.133

Table 3 Embedded heat pipes resistances at 2000RPM

2000 (RPM)						
Q(W)	R_{hp1}	R_{hp2}	R_{hp3}	R_{hp4}	R_{hp5}	R_{hp6}
30	0.274	0.335	0.322	0.392	0.512	0.285
60	0.274	0.262	0.268	0.294	0.384	0.219
90	0.260	0.223	0.215	0.228	0.341	0.204
120	0.253	0.204	0.193	0.220	0.304	0.186
150	0.253	0.205	0.189	0.215	0.282	0.184
180	0.221	0.181	0.172	0.130	0.213	0.153
210	0.220	0.167	0.153	0.147	0.219	0.153
240	0.226	0.159	0.153	0.159	0.248	0.167
270	0.225	0.158	0.152	0.163	0.249	0.173
300	0.198	0.161	0.141	0.127	0.230	0.146

Table 4 Embedded heat pipes resistances at 1000RPM

1000 (RPM)						
Q(W)	R_{hp1}	R_{hp2}	R_{hp3}	R_{hp4}	R_{hp5}	R_{hp6}
30	0.421	0.416	0.411	0.705	0.866	0.356
60	0.335	0.274	0.274	0.480	0.600	0.262
90	0.281	0.214	0.215	0.363	0.488	0.216
120	0.263	0.208	0.196	0.288	0.383	0.193
150	0.241	0.185	0.172	0.243	0.360	0.176
180	0.236	0.192	0.169	0.267	0.344	0.192
210	0.224	0.178	0.162	0.265	0.342	0.176
240	0.210	0.170	0.154	0.200	0.300	0.162
270	0.223	0.174	0.159	0.192	0.288	0.170
300	0.214	0.170	0.149	0.173	0.273	0.163

Table 5 R_{bhp} resistances at 3000 RPM

3000 (RPM)						
Q(W)	R_{bhp1}	R_{bhp2}	R_{bhp3}	R_{bhp4}	R_{bhp5}	R_{bhp6}
30	0.666	0.640	0.636	1.060	1.594	0.649
60	0.635	0.651	0.636	1.090	1.570	0.660
90	0.611	0.625	0.621	1.070	1.545	0.649
120	0.609	0.618	0.619	1.068	1.509	0.638
150	0.616	0.618	0.609	1.048	1.497	0.632
180	0.625	0.614	0.614	1.040	1.489	0.627
210	0.636	0.624	0.626	1.056	1.511	0.643
240	0.666	0.645	0.644	1.075	1.545	0.657
270	0.669	0.664	0.660	1.101	1.583	0.661
300	0.696	0.673	0.672	1.110	1.600	0.681

Table 6 R_{bhp} at 2000 RPM

2000 (RPM)						
Q(W)	R_{bhp1}	R_{bhp2}	R_{bhp3}	R_{bhp4}	R_{bhp5}	R_{bhp6}
30	0.696	0.608	0.623	1.813	2.179	0.657
60	0.622	0.576	0.580	1.691	1.987	0.625
90	0.611	0.573	0.587	1.699	1.965	0.621
120	0.601	0.566	0.580	1.666	1.923	0.614
150	0.594	0.553	0.567	1.627	1.897	0.596
180	0.625	0.573	0.584	1.715	1.976	0.632
210	0.608	0.560	0.574	1.638	1.895	0.604
240	0.606	0.568	0.575	1.642	1.867	0.594
270	0.607	0.563	0.571	1.623	1.851	0.584
300	0.632	0.563	0.582	1.681	1.916	0.625

Table 7 R_{bhp} at 1000 RPM

1000 (RPM)						
Q(W)	R_{bhp1}	R_{bhp2}	R_{bhp3}	R_{bhp4}	R_{bhp5}	R_{bhp6}
30	0.689	0.606	0.647	2.884	2.533	0.733
60	0.565	0.530	0.549	2.435	2.133	0.628
90	0.549	0.505	0.522	2.307	2.000	0.601
120	0.546	0.492	0.519	2.275	1.983	0.587
150	0.551	0.488	0.509	2.269	1.960	0.587
180	0.555	0.486	0.516	2.232	1.944	0.569
210	0.530	0.468	0.490	2.124	1.857	0.554
240	0.553	0.478	0.497	2.203	1.908	0.568
270	0.549	0.473	0.496	2.215	1.911	0.563
300	0.553	0.479	0.503	2.243	1.940	0.572

Table 8 R_{hpa} at 3000 RPM

3000 (RPM)						
Q(W)	R_{hpa1}	R_{hpa2}	R_{hpa3}	R_{hpa4}	R_{hpa5}	R_{hpa6}
30	0.125	0.176	0.175	0.242	0.483	0.194
60	0.114	0.165	0.164	0.212	0.458	0.184
90	0.097	0.161	0.168	0.202	0.467	0.173
120	0.125	0.198	0.208	0.227	0.507	0.189
150	0.116	0.198	0.210	0.230	0.512	0.190
180	0.111	0.195	0.212	0.222	0.499	0.187
210	0.110	0.198	0.213	0.225	0.496	0.185
240	0.109	0.204	0.216	0.231	0.501	0.189
270	0.108	0.206	0.221	0.235	0.515	0.199
300	0.109	0.209	0.220	0.233	0.505	0.188

Table 9 R_{hpa} at 2000 RPM

2000 (RPM)						
Q(W)	R_{hpa1}	R_{hpa2}	R_{hpa3}	R_{hpa4}	R_{hpa5}	R_{hpa6}
30	0.168	0.188	0.215	0.441	0.769	0.241
60	0.147	0.199	0.215	0.441	0.801	0.241
90	0.154	0.223	0.243	0.457	0.812	0.241
120	0.168	0.246	0.268	0.490	0.881	0.263
150	0.160	0.243	0.271	0.500	0.884	0.267
180	0.172	0.258	0.283	0.522	0.908	0.274
210	0.153	0.248	0.273	0.497	0.870	0.263
240	0.174	0.272	0.298	0.539	0.945	0.285
270	0.159	0.263	0.286	0.517	0.911	0.272
300	0.162	0.262	0.288	0.500	0.871	0.261

Table 10 R_{hpa} at 1000 RPM

1000 (RPM)						
Q(W)	R_{hpa1}	R_{hpa2}	R_{hpa3}	R_{hpa4}	R_{hpa5}	R_{hpa6}
30	0.172	0.246	0.254	0.705	1.066	0.314
60	0.191	0.274	0.294	0.737	1.066	0.304
90	0.217	0.315	0.333	0.833	1.155	0.328
120	0.234	0.331	0.352	0.929	1.266	0.361
150	0.233	0.340	0.368	0.923	1.253	0.360
180	0.252	0.353	0.382	0.993	1.344	0.380
210	0.240	0.338	0.366	0.943	1.266	0.359
240	0.241	0.345	0.377	0.961	1.291	0.369
270	0.259	0.372	0.400	1.047	1.392	0.396
300	0.258	0.365	0.398	1.019	1.360	0.387

CONCLUSION

The thermal modules of embedded heat pipes were well evaluated through careful experimenting and fitted for electronic cooling in this article. Intentionally, fan should be kept above a certain speed over 1000 RPM to obtain better cooling efficiency. The heat flow ratio of total heat flow through the heat pipe is also different under variable heat source areas. The total thermal resistances remain fairly constant at the dual fans speeds of 1000 RPM and above input power of 90 W. The differences of total thermal resistances between fan speeds of 2000 RPM and 3000 RPM are almost non-existing; the thermal module has well thermal performance at 2000 RPM. Total thermal resistances were affected by heat source areas. The smaller they had large variation of the heating power resulting from higher heat flux causing the heat pipe to reach its operating limits more easily. Due to these heat pipes embedded into based plate take away heat flow from heat source, the thermal performance of thermal module stays the same at input power of 300 W. That is, the total thermal resistance varies according to the functionality of the embedded heat pipes. Finally, a method of thermal performance solution of the model is established in the present paper.

ACKNOWLEDGMENTS

This paper originally appeared in the Conference and Publication of Taiwan Thermal Management Association (TTMA) and others utilizing Chinese language and is a major revised version. Some of the materials presented in the present paper were first published in TTMA and others. The author gratefully acknowledges TTMA and others for their guidance on preparation of this manuscript to publish in Chinese language and permission to reprint the materials here. Finally, the author would like to thank all of his colleagues and students who contributed to this study.

REFERENCES

[1] J.-C. Wang et al (2007) Experimental Investigations of Thermal Resistance of a Heat Sink with Horizontal Embedded Heat Pipes. International Communications in Heat and Mass Transfer 34: 958-970. doi:10.1016/j.icheatmasstransfer.2007.03.015

[2] T.S.Liang and Y.M. Hung 2010, Experimental investigation on the thermal performance and optimization of heat sink with U-shape heat pipes, ENERGY CONVERSION AND MANAGEMENT, 51, Issue 11, 2109-2116.

[3] J.-C. Wang, R.-T. Wang, C.-C. Chang, C.-L. Huang 2010, Program for Rapid Computation of the Thermal Performance of a Heat Sink with Embedded Heat Pipes, JOURNAL OF THE CHINESE SOCIETY OF MECHANICAL ENGINEERS, 31, Issue 1, 21-28.

[4] Y.-W. Chang et al (2008) Heat Pipe for Cooling of Electronic Equipment. Energy Conversion and Management. 49:3398-3404. doi:10.1016/j.enconman.2008.05.002

[5] E. Azad (2012) Predict the temperature distribution in gas-to-gas heat pipe heat exchanger. Heat and Mass Transfer 48:1177–1181.

[6] T. Kaya and J. Goldak (2007) Three-dimensional numerical analysis of heat and mass transfer in heat pipes. Heat Mass Transfer 43:775–785.

[7] A. I. Uddin and C. M. Feroz (2009) Effect of working fluid on the performance of a miniature heat pipe system for cooling desktop processor. Heat and Mass Transfer 46:113–118.

[8] J.-C. Wang and S.-L. Chen (2011), Air Cooling Module Applications to Consumer-Electronic Products, InTech Open Access Publisher, Chapter 14 pp.339-366. (http://www.intechopen.com/articles/show/title/air-cooling-module-applications-to-consumer-electronic-products).

[9] T.-E. Tsai et al (2010) Dynamic test method for determining the thermal performances of heat pipes. International Journal of Heat and Mass Transfer 53:4567-4578.

[10] A. A. El-Nasr and S. M. El-Haggar (1996) Effective thermal conductivity of heat pipes. Heat Mass Transfer 32:97-101.

[11] R.-T. Wang et al (2011) Experimental Analysis for Thermal Performance of a Vapor Chamber Applied to High-Performance Servers. Journal of Marine Science and Technology-Taiwan 19: 353-360.

[12] S.W. Chi, 1976, Heat pipe theory and practice: a sourcebook, 1st ed., Hemisphere Pub. Corp., Chapter 1, pp.1-30.

[13] J.-C. Wang (2011) Investigations on Non-Condensation Gas of a Heat Pipe. Engineering 3: 376-383.

[14] J.-C. Wang (2011) L-type Heat Pipes Application in Electronic Cooling System. International Journal of Thermal Sciences. 50:97-105. doi:10.1016/j.ijthermalsci.2010.07.001

[15] R.-T. Wang (2013) A fitting, simple and versatile window program (HSHPTM) design using lumped parameters and one-dimensional thermal resistance models. Heat Mass Transfer 49:291–297

[16] J.-C. Wang (2009) Superposition Method to Investigate the Thermal Performance of Heat Sink with Embedded Heat Pipes. International Communication in Heat and Mass Transfer 36:686-692. doi:10.1016/j.icheatmasstransfer.2009.04.008

[17] J.-C. Wang, (2014) U- and L-shaped Heat Pipes Heat Sinks for Cooling Electronic Components Employed a Least Square Smoothing Method, Microelectronics Reliability, in press. doi:10.1016/j.microrel.2014.02.034.

[18] J.-C. Wang, (2014) L- and U-shaped Heat Pipes Thermal Modules with Twin Fans for Cooling of Electronic System under Variable Heat Source Areas, Heat and Mass Transfer, in press. http://link.springer.com/article/10.1007/s00231-014-1358-5.

[19] J.-C. Wang (2012), Computer Aided-Thermal Module Design, Nova Publisher, Chapter 1 pp.1-34. (https://www.novapublishers.com/catalog/product_info.php?products_id=31790).